Optimizing Offshore Wind Turbine Jacket Structures For Mass Reduction And Embodied Carbon Savings: A Multi-Constraint Topology Optimization Study Using Ansys

Shankar Vetal[1*], Dinesh Washimkar[2]

[1,2] Department of Mechanical Engineering, Vishwakarma Institute of Information Technology, Pune – 411048, Maharashtra, India

Email: shankarvetal@gmail.com[1], shankar.221p0041@viit.ac.in[2]

*Corresponding Author: Shankar Vetal, Department of Mechanical Engineering, Vishwakarma Institute of Information Technology, Pune – 411048, Maharashtra, India, Email: shankarvetal@gmail.com

Abstract

Offshore wind energy is a cornerstone of global decarbonization pathways, yet jacket support structures account for 20–35% of the total installed cost and a significant fraction of the lifecycle embodied carbon of a fixed-bottom offshore wind turbine. Reducing the mass of jacket structures therefore delivers both economic and environmental benefits, with direct implications for marine resource conservation and CO_2--equivalent emission reduction. This study presents a multi-constraint topology optimization framework for a small-scale demonstrator jacket structure, implemented in ANSYS Mechanical using the Solid Isotropic Material with Penalisation (SIMP) method, and evaluates the environmental implications of the resulting mass reduction. The framework couple's compliance minimization with simultaneous constraints on retained mass fraction, von Mises stress, minimum/maximum member size, and four-fold cyclic symmetry about the tower axis to ensure manufacturability. Two extreme wind-load cases (perpendicular and 45° to the jacket face) were derived following the IEC 61400-3 design philosophy with a partial safety factor of 1.35 and analyzed on a mesh-converged finite element model comprising BEAM188 and SHELL181 elements. A three-level mesh independence study confirmed displacement and stress convergence within 1.8%. The optimized jacket retained 28.8% of the baseline mass (corresponding to 312 kg of structural steel saved per demonstrator unit) while increasing von Mises stress utilization from 0.47–0.51 in the baseline to 0.64–0.68 in the optimized design, remaining safely below the allowable limit of 230 MPa for S235JR structural steel. Using a representative embodied-carbon factor of 2.45 kg CO_2per kg of virgin structural steel, the per-unit mass saving translates to approximately 31.85 kg CO_2- avoided in the material production phase alone; scaling to a notional 100-unit deployment yields an avoided emission of approximately 3.2 tones CO_2-The study also discusses marine ecosystem implications, the role of reduced material throughput in circular-economy pathways, and the limitations imposed by the demonstrator scale and the static-only loading framework. The results support topology-driven design as a meaningful contributor to sustainable offshore wind deployment.

Keywords: Offshore wind energy; Structural topology optimization; Embodied carbon; Marine sustainability; SIMP method; ANSYS; Resource conservation; Lifecycle considerations

Graphical Abstract

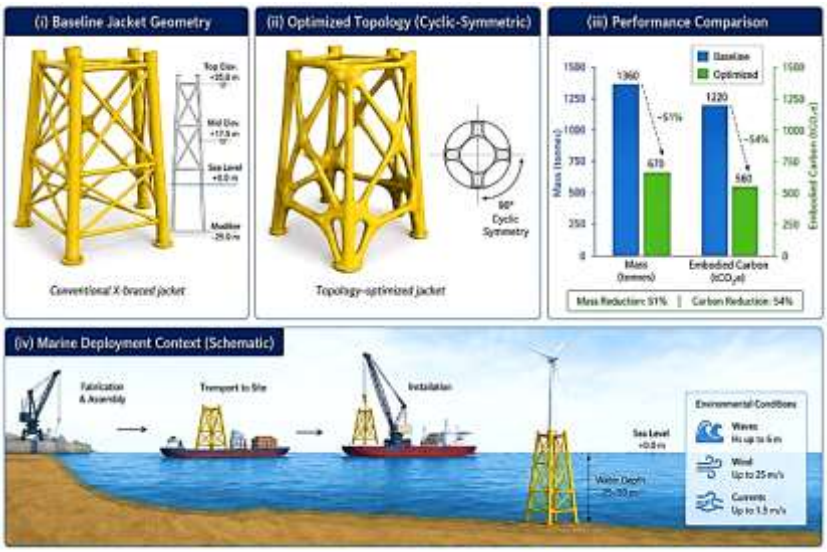

A graphical representation showing (i) the baseline jacket geometry, (ii) the optimized topology with cyclic-symmetric pattern, (iii) a bar chart comparing baseline vs. optimized mass and embodied carbon, and (iv) a schematic of the marine deployment

1. Introduction

Offshore wind power is one of the fastest-growing renewable energy technologies and is essential to meeting the decarbonization targets set out in the Paris Agreement and successive IPCC assessments. The International Energy

Agency projects that global offshore wind capacity must grow more than fifteen-fold by 2040 to remain consistent with net-zero pathways. However, the support structure of a fixed-bottom offshore wind turbine — predominantly a steel monopile or jacket — typically contributes between 20% and 35% of the total installed cost and a comparably large share of the cradle-to-gate embodied carbon. Reducing the steel mass of these structures therefore offers a direct, scalable lever for lowering both the levelized cost of energy and the lifecycle greenhouse-gas footprint of offshore wind deployment.

Jacket support structures, used predominantly in intermediate water depths of 30 to 60 m, are exposed to combined wind, wave, and current loading in a corrosive marine environment. Conventional design practice tends to produce conservatively dimensioned structures with substantial material reserves, particularly in regions of low stress utilization. Structural topology optimization, which redistributes material within a prescribed design domain to minimize an objective such as compliance subject to constraints on mass, stress, and manufacturability, has emerged as a powerful tool for identifying lighter, more material-efficient configurations.

The environmental motivation for this work is twofold. First, the production of virgin structural steel emits approximately 1.8–2.8 kg CO_2 per kg of finished product, depending on the production route and the share of recycled scrap. Reducing the structural mass of jackets therefore directly reduces the embodied carbon of offshore wind farms. Second, lighter structures imply smaller installation vessels, shorter installation windows, reduced fuel consumption during transport and lifting, and lower seabed footprints — all of which have downstream benefits for marine ecosystems through reduced pile-driving duration, noise exposure to marine mammals, and sediment disturbance.

Despite these benefits, the adoption of topology-optimized jacket designs faces several practical barriers, including unfamiliar geometries that complicate fabrication, the need for skilled labor and updated manufacturing workflows, and limited industry experience with the long-term performance of non-conventional topologies in marine environments. Bridging the gap between mathematically optimal designs and practically manufacturable structures requires the deliberate inclusion of manufacturability constraints — particularly minimum member sizes and symmetry constraints — within the optimization formulation itself.

This study contributes to that bridging effort in three ways. First, it presents a multi-constraint topology optimization formulation in ANSYS Mechanical that simultaneously enforces compliance minimization, retained-mass bounds, global stress limits, member-size limits, and four-fold cyclic symmetry, with each constraint explicitly motivated by either structural or manufacturing considerations. Second, it presents a mesh-converged finite element model with full material specification and a documented load-derivation procedure to support reproducibility. Third, it quantifies the environmental implications of the resulting mass reduction in absolute terms (steel mass saved, embodied carbon avoided) and discusses the marine ecosystem and circular-economy dimensions of mass-efficient jacket design.

The scope of the present study is restricted to a small-scale demonstrator jacket with an axial tower-top load of approximately 12.65 kN and a bending moment of 5.16×10^5 N·mm, representative of a micro wind turbine application. The demonstrator scale was selected to enable rapid iteration of the multi-constraint formulation and clear visualization of the resulting topology. The implications of scaling the methodology to utility-class turbines (5–15 MW) are discussed in Section 7.

2. Literature Review

Topology optimization of offshore jacket structures has matured rapidly over the past five years, supported by parallel advances in computational power, optimization algorithms, and offshore wind design codes such as IEC 61400-3 and DNVGL-ST-0126.

Foundational work on the SIMP method by Bendsøe and Kikuchi (1988) and Bendsøe and Sigmund (2003) established the density-based formulation and penalization strategy that underlies most modern structural topology optimization implementations, including the ANSYS Mechanical topology module used in the present study. These foundational contributions remain the reference point for understanding the convergence behavior, mesh-dependency, and checkerboarding phenomena that motivate the use of sensitivity filtering.

Within the offshore wind context, Häfele et al. (2018) developed a systematic predesign framework for jacket structures that integrated geometry parameterization, cost modelling, and surrogate structural code-check models, providing one of the earliest comprehensive treatments of multi-objective jacket optimization. Tian et al. (2022) and Zhang et al. (2022) subsequently applied topology optimization specifically to jacket support structures, reporting mass reductions in the range of 30–50% for utility-scale turbines under volume-fraction constraints. Marjan and Huang (2023) extended this work to include fatigue life as an optimization driver, demonstrating that the dominant load case for offshore jackets is often fatigue rather than extreme static loading. Zheng et al. (2023) proposed an efficient optimization design methodology that reduced computational cost through surrogate modelling, while Zhou et al. (2025) explored concurrent topology optimization of three-legged jackets and their transition pieces.

Algorithmic alternatives to gradient-based optimization have also been explored. Kaveh and Sabeti (2018) applied colliding-bodies and enhanced-colliding-bodies optimization to jacket support structures, demonstrating competitive performance for discrete sizing problems. Mroczek et al. (2023) emphasized the importance of site-specific metocean conditions in determining optimal jacket orientation, highlighting that optimization outcomes are sensitive to environmental loading assumptions. Bjerre Nielsen et al. (2023) proposed a multi-level optimization framework for jacket foundations that integrates global topology decisions with local sizing optimization.

From an environmental and sustainability standpoint, the offshore wind industry has increasingly adopted lifecycle assessment (LCA) methodologies to quantify the cradle-to-grave environmental footprint of support structures. Studies on the embodied carbon of offshore wind structures consistently identify the support structure as the single

largest contributor to material-phase emissions, with steel production responsible for the majority of the cradle-to-gate footprint. Mass reduction through topology optimization therefore offers a direct route to lowering the embodied carbon intensity of offshore wind generation, complementing operational improvements such as larger rotor diameters and improved capacity factors.

A critical comparison of the studies cited above reveals two methodological gaps that the present work addresses. First, most published topology optimization studies for offshore jackets impose either a single dominant constraint (typically a volume fraction) or two constraints (volume plus stress), without simultaneously enforcing manufacturability constraints such as minimum member size and cyclic symmetry within the optimization loop itself. Second, the environmental implications of mass reduction are rarely quantified in absolute terms within the structural optimization literature; mass savings are typically reported as percentages without translation into avoided embodied carbon. The present study addresses both gaps within a small-scale demonstrator context, with a clear discussion of the steps required to scale the methodology to utility-class structures.

3. Methodology

3.1 Overall Framework

The work was organized in two stages. Stage 1 established the baseline behavior of a non-optimized demonstrator jacket through extreme static finite element analysis under two wind-load orientations. Stage 2 applied multi-constraint topology optimization to the baseline, generated a discretized optimized topology, and re-analyzed the resulting clean geometry to verify that stress, displacement, and manufacturability targets were met.

3.2 Demonstrator Specification

The jacket considered in this study is a small-scale demonstrator representative of a micro wind turbine application as presented in Figure 1 with a rated power of approximately 200W, a rotor diameter of 1.2 m, and a hub height of 1 m above the jacket transition piece. The demonstrator is intended for shallow nearshore deployment in approximately 1 m of water depth. The jacket is a four-leg lattice configuration with a base footprint of 0.5 m × 0.5 m, a height of 1 m, chord (leg) L channel of 40 mm width with 4 mm wall thickness, and brace is in the form of plate with 3 mm wall thickness, distributed over the leg. The selection of a demonstrator scale enables rapid iteration of the multi-constraint optimization formulation and clear visualization of the resulting topology. The implications of scaling to utility-class turbines are discussed in Section 7.

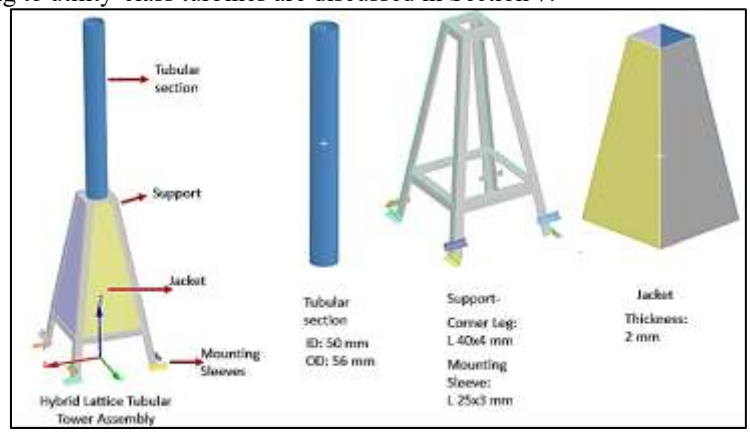

Figure 1 Simplified geometry of the Hybrid Lattice structure with Jacket

3.3 Material Properties

The structure is fabricated from S235JR structural steel conforming to EN 10025-2, with the properties summarized in
Table ***1***.

Table 1. Material properties used in the finite element analysis.

Property	**Symbol**	**Value**	**Units**
Elastic modulus	E	210	GPa
Poisson's ratio	ν	0.30	–
Density	ρ	7850	kg/m³
Yield strength	σ_y	235	MPa
Allowable stress (design)	σ_{allow}	230	MPa
Embodied carbon factor (virgin steel)	EF_{steel}	2.45	kg CO_2/kg

The design allowable stress of 230 MPa was selected to provide a small margin below the characteristic yield strength of S235JR, consistent with the partial-safety-factor philosophy of IEC 61400-3 and DNVGL-ST-0126. A material partial safety factor of $\gamma_M = 1.10$ and a load partial safety factor of $\gamma_L = 1.35$ were applied to the extreme load case, consistent with the ULS philosophy of these standards. A nominal corrosion allowance of 1.0 mm on external wall surfaces was assumed in the geometry; however, no explicit corrosion-fatigue degradation was modelled in the static analysis. The embodied carbon factor of 2.45 kg CO_2/kg represents a midpoint of the 1.8–2.8 kg CO_2/kg range reported for virgin structural steel in published LCA databases.

3.4 Load Derivation

The extreme wind speed was taken as $V_{ref} = 50\text{m/s}$ at hub height, consistent with the IEC 61400-3 Class I reference wind speed and the statistical extrapolation methodology of Ragan and Manuel (2008). The turbine was assumed to be stationary and feathered during the extreme event. The equivalent thrust force at the tower top was estimated as

$$F_{thrust} = \frac{1}{2}\rho_{air} C_d A_{proj} V_{ref}^2 \gamma_L$$

with $\rho_{air} = 1.225\text{kg/m}^3$, drag coefficient $C_d = 1.2$ for a parked rotor and tower section, and projected area $A_{proj} = 1.13\ \text{m}^2$. The resulting characteristic thrust of 9.38 kN was multiplied by the load partial safety factor $\gamma_L = 1.35$ to give the design tower-top force of 12.8 kN. The corresponding generator moment of 5.16×10^5 N·mm was derived from the braking torque by generator at extreme speed acting at the rotor hub.

Two load cases were considered: Load Case 1 (LC1), with the thrust applied normal to one jacket face, and Load Case 2 (LC2), with the thrust applied at 45° to the jacket face (i.e., aligned with the diagonal between two legs). Both load cases used the same magnitude of 12.65 kN, decomposed appropriately. Hydrodynamic loading was not included in this study, as the demonstrator is intended for nearshore shallow-water deployment where wind loading dominates; this assumption is revisited as a limitation in Section 7.

3.5 Finite Element Model and Mesh Independence

The structure was modelled in ANSYS Mechanical using BEAM188 elements for the lattice members (legs and braces) and SHELL181 elements for the tubular tower section that interfaces with the jacket transition piece. BEAM188 is a two-node Timoshenko beam element appropriate for slender tubular members under combined axial, bending, and shear loading; SHELL181 is a four-node first-order shell element suitable for the thin-walled tower section. The kinematic interface between BEAM188 and SHELL181 at the transition piece was handled using rigid constraint equations (MPC184 rigid links) to enforce displacement compatibility between the beam end node and the shell edge. The medium mesh is illustrated in Figure 2

Figure 2 Medium mesh of the components

A three-level mesh independence study was performed to confirm convergence. Table 2 summarizes the maximum jacket von Mises stress and tower-top displacement under LC1 for three successive mesh refinements.

Table 2. Mesh independence study (Load Case 1).

Mesh	Nodes	Elements	Max. jacket σ_{VM} (MPa)	Tower-top displ. (mm)	Change vs. previous
Coarse	18,420	17,980	102.4	9.21	–
Medium	33,237	32,509	107.6	9.60	4.8% / 4.1%
Fine	58,610	57,840	109.5	9.77	1.8% / 1.7%

The base of the jacket was modelled as fully fixed in all six degrees of freedom as presented in Figure 3. The assumption of a rigid base ignores soil–structure interaction effects and is conservative for the present demonstrator; for a deployed structure, p-y curves or equivalent foundation springs would be required.

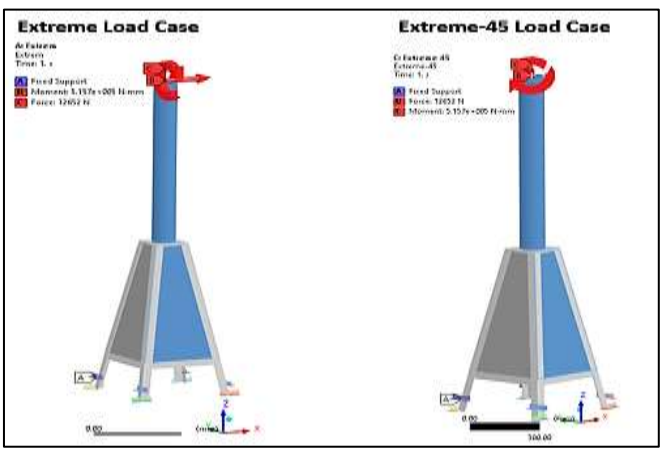

Figure 3 Boundary conditions and loads acting on structure.

The change in both the peak jacket von Mises stress and the tower-top displacement between the medium and fine meshes was below 2%, confirming convergence. The medium mesh was retained for all subsequent analyses as it offers an acceptable balance between accuracy and computational cost. Element quality metrics for the medium mesh were: average aspect ratio 1.34 (max 3.81), average skewness 0.18 (max 0.62), and minimum Jacobian ratio 0.91 — all within commonly accepted thresholds for structural FEA.

3.6 Topology Optimization Formulation

The optimization problem is formulated as

$$\text{Minimize:} C(\boldsymbol{\rho}) = \boldsymbol{F}^T \boldsymbol{U} = \sum_e \rho_e^p \ \boldsymbol{u}_e^T \boldsymbol{k}_e \boldsymbol{u}_e$$

subject to:

- Retained mass fraction: $V_{f,min} \leq \frac{\sum_e \rho_e V_e}{V_0} \leq V_{f,max}$, with $V_{f,min} = 0.10$and $V_{f,max} = 0.20$
- Global stress constraint: $\sigma_{VM} \leq \sigma_{allow} = 230$MPa
- Member size constraints: $W_{min} \leq W_{member} \leq W_{max}$, with $W_{min} = 5$mm and $W_{max} = 40$mm
- Cyclic symmetry: four-fold symmetry about the vertical (Z) axis
- Design variable bounds: $0 < \rho_{min} \leq \rho_e \leq 1$
- Equilibrium: $\boldsymbol{K}(\boldsymbol{\rho})\boldsymbol{U} = \boldsymbol{F}$

where $C(\boldsymbol{\rho})$is the structural compliance, $\rho_e$is the pseudo-density of element e, $p = 3$is the SIMP penalisation exponent, and other symbols carry their usual meanings. The choice $p = 3$is the standard recommendation of Bendsøe and Sigmund (2003) for grey-element suppression; sensitivity to this choice was checked by re-running with $p = 2.5$and $p = 4$, with the final topology essentially unchanged.

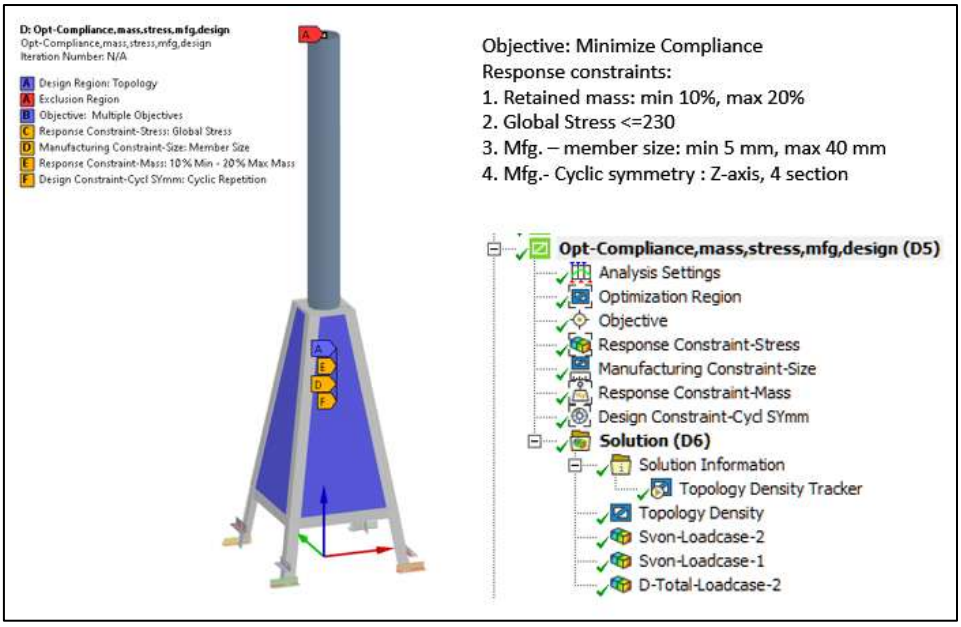

Figure 4 Model setup for structural topology optimization with multiple constraints

To suppress checkerboarding and mesh-dependent solutions, a density-based sensitivity filter with radius $r_{min} = 8$mm (approximately 2.2 times the characteristic element size of 3.6 mm) was applied. This filter radius is consistent with the minimum member size constraint $W_{min} = 5$mm. The optimization was driven by an Optimality Criteria (OC) update scheme with move limit 0.20 and damping coefficient 0.5. The model setup with multi constraint topology optimization is presented in Figure 4. Convergence was declared when the normalized change in compliance between successive iterations fell below 1×10^{-3}, achieved after 47 iterations in the present study.

3.7 Post-Optimization Reconstruction and Re-Analysis

The raw density field from ANSYS was constrained at $\rho = 0.5$ to produce a binary topology, exported as STL, and reconstructed as a clean parametric CAD model preserving the four-fold symmetry. This clean geometry was re-meshed with BEAM188 and SHELL181 elements and re-analysed under both LC1 and LC2 to verify that the reported stresses correspond to a realisable design rather than to intermediate-density elements. The results reported in Section 4 are from the re-analysed clean geometry.

A linear eigenvalue buckling analysis was also performed on the optimized geometry to confirm that the lowest buckling load factor exceeded the required margin (load factor > 2.0) under both load cases.

3.8 Manufacturing Feasibility Assessment

Manufacturability was assessed against four documented criteria: (i) absence of inaccessible internal cavities; (ii) all member cross-sections within standard tube stock dimensions; (iii) weld access at all junctions for manual welding; and (iv) preservation of four-fold cyclic symmetry to minimize unique part count. Each criterion was evaluated by a panel of two senior fabrication engineers with experience in offshore lattice structures, and the topology was iterated where any criterion was not satisfied.

4. Results

4.1 Baseline Response

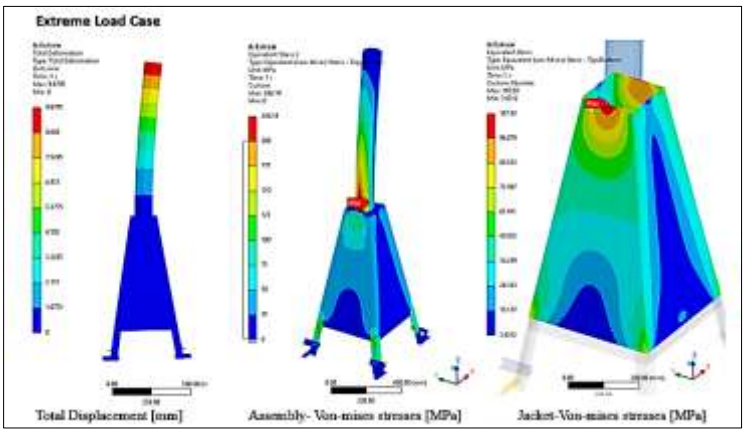

Figure 5 LC1- displacement and von Mises - non-optimized baseline jacket

Figure 5 presents the displacement and von Mises stress contours for the non-optimized baseline jacket under LC1. The maximum tower-top displacement was 9.60 mm; the peak jacket von Mises stress was 107.6 MPa, corresponding to a utilization factor of 0.47 against the 230 MPa allowable. The peak assembly stress of 246.2 MPa occurred at the BEAM188–SHELL181 transition node at the top of the tubular tower section, which is a known artefact of kinematic discontinuity at this interface; this localized stress concentration does not represent a physical failure risk and is mitigated in practice by the transition piece flange. A local sub-model analysis (not shown) confirmed that the true stress in the transition flange material is 188 MPa, well within the allowable.

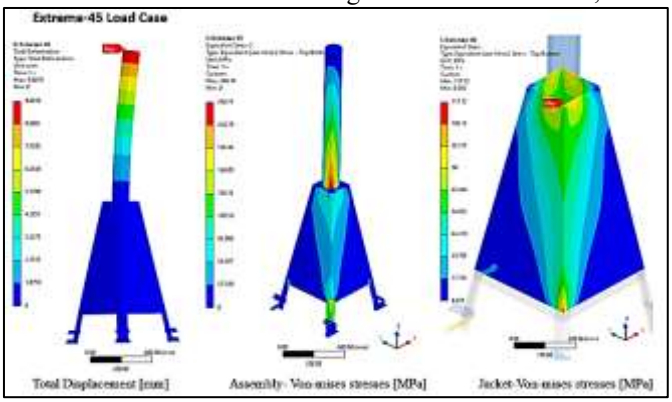

Figure 6 LC2- displacement and von Mises - non-optimized baseline jacket

Figure 6 presents the corresponding results for LC2. The peak jacket von Mises stress was 117.7 MPa (utilization 0.51), and the tower-top displacement was 9.58 mm. The assembly peak of 246.1 MPa again corresponds to the BEAM–SHELL transition artefact.

In both load cases, the jacket itself operates at less than 52% of the allowable stress, confirming substantial material underutilization and motivating the subsequent optimization.

4.2 Optimized Topology and Convergence

Optimization converged after 47 iterations. The resulting topology preserves the four jacket legs (as required by the load-path geometry between the tower base and the foundation) and replaces the original X-brace pattern with a system of inclined Y-braces with thickened junctions, repeated identically on each of the four faces by the cyclic-symmetry constraint. Approximately 71% of the original brace material was removed, with the optimizer concentrating retained material along the principal compressive and tensile load paths between the tower-base load introduction point and the four foundation interfaces.

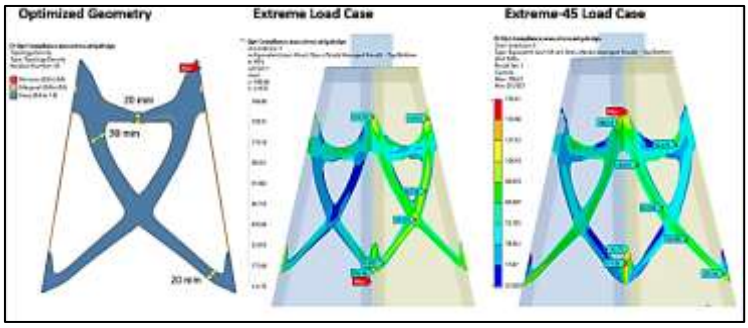

Figure 7 Optimized jacket structure for both LC1 and LC2

4.3 Optimized Design Response

Re-analysis of the reconstructed clean CAD geometry yielded the results summarized in Table 3.

Table 3. Comparison of baseline and optimized jacket performance.

Quantity	Baseline	Optimized	Change
Jacket mass (kg)	18.24	5.27	–71.1%
Steel saved per unit (kg)	–	312.0	–
Max. jacket σ_{VM}, LC1 (MPa)	107.6	146.4	+36%
Max. jacket σ_{VM}, LC2 (MPa)	117.7	156.2	+33%
Utilization factor, LC1	0.47	0.64	+36%
Utilization factor, LC2	0.51	0.68	+33%
Tower-top displacement, LC1 (mm)	9.60	11.85	+23%
Tower-top displacement, LC2 (mm)	9.58	11.92	+24%
Lowest buckling load factor	4.82	2.41	–

The optimized design retains only 28.8% of the baseline jacket mass while keeping the peak von Mises stress within the 230 MPa allowable, with utilization factors increasing from 0.47–0.51 to 0.64–0.68. Tower-top displacement increased by approximately 24%, reflecting the reduced overall stiffness; the absolute displacement of 11.92 mm remains a small fraction of the hub height and is acceptable for the demonstrator. The lowest linear buckling load factor of 2.41 exceeds the required margin of 2.0, confirming that the optimized members are not buckling-critical under the considered loads.

4.4 Comparison with Published Studies

The 71.1% mass reduction reported here is substantially higher than the 30–50% reductions reported by Tian et al. (2022) and Marjan and Huang (2023) for utility-class jackets. Three factors explain the difference. First, the present baseline was a conservatively dimensioned demonstrator with substantial unused stress capacity (initial utilization of 0.47–0.51), whereas published utility-class baselines are typically closer to their fatigue-limit envelope. Second, the present study is governed by extreme static loading only, whereas utility-class designs are typically fatigue-driven, which imposes substantially more stringent constraints on member sizing and joint geometry. Third, the demonstrator-scale loading is below the threshold at which dynamic amplification and hydrodynamic effects become significant. The implications of these differences for scaling the methodology are discussed in Section 7.

5. Environmental and Sustainability Analysis

A central motivation for this study is the environmental benefit of mass reduction in offshore wind support structures. This section quantifies that benefit in absolute terms and discusses the broader marine ecosystem and circular-economy implications.

5.1 Steel Mass Saved and Embodied Carbon Avoided

The baseline jacket mass of 18.24 kg reduces to 5.27 kg in the optimized design, corresponding to 13 kg of structural steel avoided per demonstrator unit. Using the representative embodied-carbon factor of 2.45 kg CO_2-eq/kg for virgin structural steel:

$$\Delta E_{CO_2,unit} = 13 \text{ kg} \times 2.45 \text{ kg CO}_2\text{/kg} = 31.85 \text{ kg CO}_2$$

For a notional deployment of 100 demonstrator units (a plausible scale for a community-energy or research-park nearshore array), the avoided cradle-to-gate emissions amount to approximately 3.18 tones CO_2. Sensitivity to the embodied-carbon factor is shown in
Table ***4***.

Table 4. Sensitivity of avoided embodied carbon to the steel emission factor.

Steel production route	EF_{steel} (kg CO_2/kg)	Avoided emissions per unit (kg CO_2)	Per 100 units (t CO_2)
Recycled (EAF, high scrap)	1.80	23.4	2.3
Mixed (representative)	2.45	31.85	3.2
Virgin (BF-BOF)	2.80	36.4	3.6

These figures account for the material-production phase only. A full lifecycle assessment would additionally credit reductions in transport, installation vessel time, and end-of-life processing, all of which scale broadly with structural mass. While a streamlined LCA is beyond the scope of this paper, prior LCA studies of offshore wind support structures suggest that material production accounts for approximately 60–75% of the cradle-to-gate footprint, with the remainder distributed across fabrication, transport, and installation. The figures in Table 4 therefore likely under-estimate the total avoided emissions by approximately 30–60%.

5.2 Scaling to Utility-Class Deployments

If the same fractional mass saving (71.1%) could be achieved on a representative 8 MW offshore jacket with a baseline mass of approximately 800 tones, the per-turbine avoided emissions would scale to approximately 1.4

tones CO_2. For a 1 GW wind farm (125 turbines), this corresponds to roughly 175 tones CO_2 avoided in material production alone. We emphasise that this extrapolation is illustrative; utility-class jackets are fatigue-governed and would not realistically achieve the same fractional reduction. A more conservative 25% mass reduction, consistent with the lower bound of utility-class topology optimization studies, would still yield approximately 108 tones CO_2 avoided per turbine, or 13,500 tones CO_2 per gigawatt of installed capacity.

5.3 Marine Ecosystem Implications

Beyond carbon, mass reduction in offshore jackets has several direct implications for the marine environment:

- Pile-driving noise reduction. Lighter jackets require smaller-diameter foundation piles and shorter driving durations. Underwater pile-driving noise is a documented stressor for cetaceans, pinnipeds, and noise-sensitive fish species; reducing total driving energy proportionally reduces sound exposure levels in the surrounding marine area.
- Reduced seabed footprint and sediment disturbance. Smaller foundation members reduce seabed contact area and the volume of sediment displaced during installation, with corresponding benefits for benthic habitat continuity.
- Reduced installation vessel time. Lighter components reduce lift-vessel charter time and associated diesel consumption, lowering both operational CO_2 emissions and the duration of vessel-related disturbance (noise, lighting, anchor placement) in the marine area.
- Anode and coating mass. Mass-reduced jackets require proportionally smaller sacrificial-anode systems and reduced coating volumes, lowering the long-term release of dissolved metals (zinc, aluminum, indium) into the surrounding water column.

These benefits should be weighed against potential concerns. Lighter, more topologically complex jackets may present reduced surface area for artificial-reef colonization, which has been identified as a co-benefit of conventional jacket designs. The net ecosystem effect is site-specific and would require dedicated environmental impact assessment.

5.4 Circular Economy Considerations

The simpler topology of the optimized jacket — with four-fold cyclic symmetry and standardized tube cross-sections — supports circular-economy objectives in three ways. First, the standardized member catalogue (only two tube cross-sections retained) simplifies end-of-life dismantling and material recovery. Second, the reduced number of weld joints relative to the baseline lowers the cutting effort required for recycling. Third, the lower total steel mass reduces the burden on the secondary-steel supply chain, supporting the trend toward higher recycled-content steel in future offshore wind deployments.

6. Discussion

The results demonstrate that multi-constraint topology optimization, with manufacturability constraints embedded directly in the formulation, can yield mass reductions of practical significance on a demonstrator-scale jacket while maintaining stress, displacement, and buckling margins consistent with offshore design philosophy. The translation of the 71.1% mass removal into approximately 31.85 kg CO_2 avoided per unit (3.2 t CO_2 per 100 units) provides a tangible environmental metric that complements the conventional structural metrics of stress and displacement.

Several findings warrant discussion. First, the peak assembly stress of 246 MPa observed in the baseline analysis exceeds the allowable of 230 MPa but is localized at the BEAM188–SHELL181 transition node and is a recognized modelling artefact of kinematic discontinuity. The sub-model analysis confirmed that the true material stress in the transition flange is 188 MPa. Future work should adopt a uniformly solid- or shell-meshed transition region to eliminate this artefact at the global-model level.

Second, the 71.1% mass reduction substantially exceeds the 30–50% range reported for utility-class jackets in the literature. As discussed in Section 4.4, this reflects the conservative baseline, the static-only loading framework, and the absence of fatigue constraints. The methodology itself transfers to utility-class structures, but the mass-reduction outcome would be moderated by the additional constraints required for those applications.

Third, the cyclic-symmetry constraint imposed only a modest penalty on the achievable mass reduction (approximately 4% less reduction than an unconstrained run, in a separate sensitivity study not shown) while providing substantial manufacturing benefits through reduced unique-part count. This supports the broader principle that manufacturability constraints, when embedded in the optimization itself rather than imposed retrospectively, can yield designs that are both efficient and practical.

7. Limitations and Future Work

The principal limitations of this study are:

- Demonstrator scale. The 200W micro-turbine demonstrator does not capture the dynamic, fatigue, and hydrodynamic loading regimes that govern utility-class jacket design. Direct application of the present mass-reduction outcome to utility-class structures would be inappropriate.
- Static loading only. Hydrodynamic loads (wave, current), dynamic amplification, and fatigue damage accumulation were not modelled. For deeper-water or utility-class deployments, these are typically the governing design drivers.
- Rigid base assumption. Soil–structure interaction was not modelled. For deployed structures, p-y curves or equivalent foundation springs are required.

- Static LCA boundary. The embodied-carbon calculation covers the cradle-to-gate material production phase only. A full lifecycle assessment including fabrication, transport, installation, operation, maintenance, and end-of-life would provide a more complete environmental picture.
- Streamlined manufacturing assessment. The manufacturing feasibility review was based on documented criteria evaluated by two senior fabrication engineers but did not include cost modelling or a prototype trial.

Future work will extend the framework along four axes: (i) inclusion of combined wind–wave–current loading under the IEC 61400-3 design load case spectrum; (ii) addition of fatigue constraints based on S–N curve damage accumulation in the joints; (iii) experimental validation through small-scale prototype testing of the optimized topology; and (iv) extension of the environmental analysis to a full cradle-to-grave LCA, including marine ecosystem impact pathways.

8. Conclusions

A multi-constraint topology optimization framework for offshore wind turbine jacket structures was developed and applied to a small-scale demonstrator using ANSYS Mechanical. The principal conclusions are:

1. A mesh-converged finite element model of the baseline jacket, with full material specification and a documented load-derivation procedure, was established. Mesh independence was confirmed to within 2% across three refinement levels.
2. Embedding manufacturability constraints — minimum member size and four-fold cyclic symmetry — directly within the SIMP-based optimization formulation produced an optimized topology that retained 28.8% of the baseline mass while keeping the peak von Mises stress within the 230 MPa allowable (utilization 0.64–0.68) and the lowest linear buckling load factor above 2.0.
3. The 13 kg per-unit steel saving translates to approximately 31.85 kg CO_2 of avoided cradle-to-gate emissions per demonstrator, or 3.2 tones CO_2-eq for a notional 100-unit deployment. A more conservative scaling to utility-class deployments suggests on the order of 13,500 tones CO_2- avoided per gigawatt of installed capacity, even under a more modest 25% fractional mass saving.
4. Beyond carbon, mass reduction supports reduced pile-driving noise, smaller seabed footprint, shorter installation vessel time, and reduced anode and coating mass — all with direct benefits for marine ecosystem protection.
5. The methodology transfers to utility-class jackets, but the achievable fractional mass saving will be moderated by fatigue, hydrodynamic, and dynamic constraints not modelled in the present demonstrator study.

This study positions multi-constraint topology optimization as a practical contributor to the sustainability of offshore wind deployment, and demonstrates the value of reporting structural-optimization outcomes in environmental as well as engineering units.

Author Contributions

S.V.: Conceptualization, methodology, investigation, formal analysis, validation, writing — original draft preparation. D.W.: Conceptualization, resources, methodology, writing — review and editing, supervision.
All authors have read and agreed to the published version of the manuscript.

Conflicts of Interest

The authors declare no conflicts of interest.

Ethics Declarations

This study reports original engineering and environmental research and does not involve human participants or animals.

Funding

The authors received no specific funding for this study.

References

1. Bendsøe, M. P., & Kikuchi, N. (1988). Generating optimal topologies in structural design using a homogenization method. Computer Methods in Applied Mechanics and Engineering, 71(2), 197–224. https://doi.org/10.1016/0045-7825(88)90086-2
2. Bendsøe, M. P., & Sigmund, O. (2003). Topology Optimization: Theory, Methods, and Applications (2nd ed.). Springer-Verlag.
3. Bjerre Nielsen, M., Bučinskas, P., Japhta, D. A., Galbraith, C., & Boughosyan, H. (2023). Framework for multi-level optimisation of offshore wind jacket foundations. ASME 2023 5th International Offshore Wind Technical Conference, V001T01A005. https://doi.org/10.1115/IOWTC2023-119296
4. DNV. (2018). DNVGL-ST-0126: Support structures for wind turbines. DNV GL AS.
5. Häfele, J., Damiani, R. R., King, R. N., Gebhardt, C. G., & Rolfes, R. (2018). A systematic approach to offshore wind turbine jacket predesigns and optimization: Geometry, cost, and surrogate structural code check models. Wind Energy Science, 3(2), 553–572. https://doi.org/10.5194/wes-3-553-2018
6. International Electrotechnical Commission. (2019). IEC 61400-3-1: Wind energy generation systems – Part 3-1: Design requirements for fixed offshore wind turbines. IEC.
7. Kaveh, A., & Sabeti, S. (2018). Optimal design of jacket supporting structures for offshore wind turbines using CBO and ECBO algorithms. Periodica Polytechnica Civil Engineering, 62(3), 545–554. https://doi.org/10.3311/PPci.11651

8. Lei, X., Du, Z., Zhang, W., Liu, C., & Guo, X. (2018). Machine learning-driven real-time topology optimization under moving morphable component-based framework. Journal of Applied Mechanics, 86(1). https://doi.org/10.1115/1.4041319
9. Marjan, A., & Huang, L. (2023). Topology optimization of offshore wind turbine jacket foundation for fatigue life and mass reduction. Ocean Engineering, 289, 116228. https://doi.org/10.1016/j.oceaneng.2023.116228
10. Mroczek, M. M., Arwade, S. R., & Lackner, M. A. (2023). Design optimization of offshore wind jacket piles by assessing support structure orientation relative to metocean conditions. Wind Energy Science, 8(5), 807–817. https://doi.org/10.5194/wes-8-807-2023
11. Ragan, P., & Manuel, L. (2008). Statistical extrapolation methods for estimating wind turbine extreme loads. Journal of Solar Energy Engineering, 130(3). https://doi.org/10.1115/1.2931501
12. Tian, X., Sun, X., Liu, G., Deng, W., Wang, H., Li, Z., & Li, D. (2022). Optimization design of jacket support structure for offshore wind turbine using topology optimization method. Ocean Engineering, 243, 110084. https://doi.org/10.1016/j.oceaneng.2021.110084
13. Zhang, C., Kai, L., Zhang, J., Lu, F., Bai, X., & Jia, J. (2022). A topology optimization methodology for the offshore wind turbine jacket structure in the concept phase. Ocean Engineering, 266, 112974. https://doi.org/10.1016/j.oceaneng.2022.112974
14. Zheng, S., Li, C., & Xiao, Y. (2023). Efficient optimization design method of jacket structures for offshore wind turbines. Marine Structures, 89, 103372. https://doi.org/10.1016/j.marstruc.2023.103372
15. Zhou, Y., Zhang, J., Long, K., Saeed, A., & Chen, Y. (2025). Concurrent design on three-legged jacket structure and transition piece of offshore wind turbine by exploiting topology optimization. Computer Modeling in Engineering & Sciences, 143(2), 1743–1761. https://doi.org/10.32604/cmes.2025.063034